Copula-Based Downscaling of Coarse-Scale Soil Moisture Observations With Implicit Bias Correction

Niko E. C. Verhoest, Martinus Johannes van den Berg, Brecht Martens, Hans Lievens, Eric F. Wood, Ming Pan, Yann H. Kerr, *Fellow, IEEE*, Ahmad Al Bitar, Sat K. Tomer, Matthias Drusch, Hilde Vernieuwe, Bernard De Baets, Jeffrey P. Walker, Gift Dumedah, and Valentijn R. N. Pauwels

***Abstract*—Soil moisture retrievals, delivered as a CATDS (Centre Aval de Traitement des Données SMOS) Level-3 product of the Soil Moisture and Ocean Salinity (SMOS) mission, form an important information source, particularly for updating land surface models. However, the coarse resolution of the SMOS product requires additional treatment if it is to be used in applications at higher resolutions. Furthermore, the remotely sensed soil moisture often does not reflect the climatology of the soil moisture predictions, and the bias between model predictions and observations needs to be removed. In this paper, a statistical framework is presented that allows for the downscaling of the coarse-scale SMOS soil moisture product to a finer resolution. This framework describes the interscale relationship between SMOS observations and model-predicted soil moisture values, in this case, using the variable infiltration capacity (VIC) model, using a copula. Through conditioning, the copula to a SMOS observation, a probability distribution function is obtained that reflects the expected distribution function of VIC soil moisture for the given SMOS observation. This distribution function is then used in a cumulative distribution function matching procedure to obtain an unbiased fine-scale soil moisture map that can be assimilated into VIC. The methodology is applied to SMOS observations over the Upper Mississippi River basin. Although the focus in this paper is on data assimilation apcations, the framework developed could also be used for other purposes where downscaling of coarse-scale observations is required.**

***Index Terms*—Hydrology, microwave radiometry, soil moisture.**

Manuscript received January 13, 2014; revised June 6, 2014, September 29, 2014, and October 30, 2014; accepted November 12, 2014. This work was supported by the ESA-ITT project "SMOS+ Hydrology Study" and by the Belgian Science Policy Office in the frame of the STEREO III program under project HYDRAS+ (SR/00/302), by the Bijzonder Onderzoeksfonds (BOF) project 01J01809, and by the CNES Terre, Océan, Surfaces Continentales, Atmosphère (TOSCA) programme.

N. E. C. Verhoest, M. J. van den Berg, B. Martens, and H. Lievens are with the Laboratory of Hydrology and Water Management, Ghent University, 9000 Ghent, Belgium (e-mail: Niko.Verhoest@UGent.be).

E. F. Wood and M. Pan are with the Department of Civil and Environmental Engineering, Princeton University, Princeton, NJ 08544 USA.

Y. Kerr, A. Al Bitar, and S. K. Tomer are with Centre d'études Spatiales de la BIOsphère (CESBIO), 31401 Toulouse, France.

M. Drusch is with the European Space Agency, European Space Research and Technology Centre (ESTEC), 2200 AG Noordwijk, The Netherlands.

H. Vernieuwe and B. De Baets are with the Department of Mathematical Modelling, Statistics and Bioinformatics, Ghent University, 9000 Ghent, Belgium.

J. P. Walker, G. Dumedah, and V. R. N. Pauwels are with the Department of Civil Engineering, Monash University, Clayton, VIC 3800, Australia.

Color versions of one or more of the figures in this paper are available online at http://ieeexplore.ieee.org.

Digital Object Identifier 10.1109/TGRS.2014.2378913

I. Introduction

MANY hydrologic processes, such as runoff production and evapotranspiration, are largely determined by the availability of soil moisture. This state variable is therefore of key importance within physically based hydrologic models, and any knowledge of its spatial distribution can be of benefit to the modeling process. Many studies have demonstrated the benefits of assimilating soil moisture observations in land surface models (LSMs) e.g., [1]–[5]. Updating soil moisture in such models with observations aims at a better modeling of the hydrologic processes affected by soil moisture, such as the partitioning of rainfall water into infiltration and runoff, and the evapotranspiration process. However, several studies have demonstrated that large systematic differences can be found between remotely sensed and modeled soil moisture [6]–[9].

The discrepancies between these different soil moisture estimates can be attributed to different causes. Not only can the remote sensing observations be biased due to errors in the retrieval algorithm [10], [11] or the effect of subgrid variability due to roads, houses, vegetation cover, etc. [8], but also due to approximations in the model structure, model parameterization and discretization, initial conditions, and errors in forcing data [10]. A further reason for the disagreement can be found in the fact that there is a vertical mismatch in the soil column between the different soil moisture products, [12], i.e., soil moisture values obtained through remote sensing are generally limited to the top few centimeters, whereas LSMs typically have a surface layer depth of 10 cm [9]. Because of these reasons, modeled soil moisture generally does not correspond well to observations, but rather shows similar trends and dynamics [13]. If, for instance, the aim of the model is to predict discharge, it may be accepted that the model state variables, such as soil moisture, diverge from the actual soil moisture states. The explanation therefore is that such discrepancies inherently compensate for poor model descriptions of hydrologic processes. In this case, soil moisture observations can be used to improve the model discharge predictions provided that the soil moisture observations are matched to the model climatology. Many studies have been devoted to addressing the discrepancies between observed and modeled soil moisture, focusing on the removal of the bias in observations or model states prior to data assimilation [6], [7], [14]–[16] or during data assimilation [10], [17]–[19].

When dealing with remote sensing products for data assimilation in spatially distributed models, another important issue is the difference in the horizontal spatial scale of the data [20]. Passive microwave sensors, such as the Advanced Microwave Scanning Radiometer—Earth Observing System [21], the Soil Moisture and Ocean Salinity (SMOS) mission [22], and the forthcoming Soil Moisture Active Passive mission [23], provide soil moisture products at a spatial resolution of tens of kilometers. In contrast, LSMs are often run at a spatial resolution of less than 10 km [9]. In literature, two approaches for assimilating data at a coarser scale have been presented. The first approach consists of *a priori* downscaling the remote sensing observations to the model scale [20], [24], [25], whereas the second approach performs a dynamic downscaling, for which innovations at the model resolution are derived from a backmapping of the difference between the coarse-scale remote sensing observations and corresponding aggregated model predictions at the coarser scale [9], [26]–[28]. It should be stated however, that, irrespective of the approach taken, assumptions have to be made on the subpixel distribution of soil moisture or on the way innovations have to be assigned to the individual subpixels. Detailed comparative studies should reveal which of the approaches and/or assumptions lead to the best update of higher resolution models given coarse-scale observations.

In the case of an *a priori* downscaling of the remote sensing observations, it is required that the remotely sensed soil moisture observations are bias corrected and rescaled prior to their assimilation into LSMs [6], [29]. In this paper, a methodology is proposed that allows for downscaling coarse-scale remotely sensed soil moisture products to the spatial scale of the LSM, accounting for differences in model climatology and bias between remotely sensed and modeled soil moisture. The resulting downscaled soil moisture product is bias corrected such that it is consistent with the model climatology. This differs from the approach of Calvet and Noilhan [30], where modeled soil moisture is scaled to the observations. Similar to Gao *et al.* [29], a copula-based joint probability distribution function is fitted to remotely sensed soil moisture observations and modeled soil moisture. However, in the current study, both data sources are not rescaled to a common spatial scale. Through conditioning the copula to a coarse-scale observation, a probability distribution function of expected soil moisture values at the model resolution is obtained for the coarse-scale remote sensing pixel considered. As the copula merely describes the dependence between both soil moisture sources, irrespective of any potential bias, this approach implicitly corrects for bias as it relates any observation with the corresponding modeled soil moisture values, each characterized by its own climatology, and also rescales the temporal variance of the observed soil moisture to that of the model. Finally, the methodology that is developed should be applicable in an operational application where coarse-scale observations are assimilated into an LSM in order to better predict discharge. To demonstrate the framework, coarse-scale SMOS soil moisture observations and finer resolution variable infiltration capacity (VIC) modeled soil moisture from the Upper Mississippi basin are used.

In this paper, a preprocessing framework is presented to downscale coarse-scale SMOS data to the finer model resolution. Although this paper does not present results from a data assimilation experiment, several advantages of the presented methodology can be listed:

1) the framework allows for a fast and simple preprocessing for obtaining a downscaled and bias-corrected product for which no explicit bias estimation is needed;
2) the framework can easily be parametrized without the need of being calibrated;
3) the bias estimation is implicitly taken into account and no bias model or assumptions with respect to the temporal and/or spatial dynamics of the bias are needed;
4) a simple data assimilation scheme can be used as no rescaling nor bias correction is needed within the data assimilation framework.

We wish to state that, although the methodology presented in this paper is framed within the context of data assimilation studies, it can also be applied for downscaling SMOS soil moisture observations (or other coarse-scale observations) based on a higher resolution map, obtained from a model, or from another remote sensing source.

II. Data Description

This study makes use of a two-year data set of SMOS Level 3 soil moisture values and corresponding VIC model simulations for the Upper Mississippi Basin. For this study, the entire data set was randomly split into two parts to allow for cross-validation. To this end, all dates were randomly assigned to one of two subsets S_1 and S_2 (each having a similar number of dates), resulting in two sets having similar soil moisture ranges for the study area. This approach avoids the problem that one data set may contain, for instance, more wet data compared with the other data set, as might occur when the time series is subdivided into two consecutive periods. In the latter case, the framework would fail, as any other data-driven method, if it were applied to data ranges that were not (well) covered in the calibration data set. However, such problem can be circumvented in an operational setting by using all preceding data to fit the copulas and regularly repeat the fitting process with new data while time is progressing. This way, the problem of applying the framework outside its region of validity is minimized. Splitting the data set into two subsets in this paper is merely done to demonstrate the validity of the method.

The following sections will describe the data set in full detail.

A. Upper Mississippi Basin

The Upper Mississippi Basin comprises portions of Minnesota, Wisconsin, Iowa, and Illinois and has an area of approximately 440 000 km^2. The basin is ideally suited as a focus area due to its large size, the lack of significant topography (which simplifies the retrieval of soil moisture from satellite observations), and the large extent of agricultural land use (e.g., corn, soybean, wheat, etc.). Moreover, there is a strong north–south precipitation gradient that ranges from approximately 475 mm/year in the north to over 1300 mm/year in the south. In the southern portion, the strong summer precipitation has

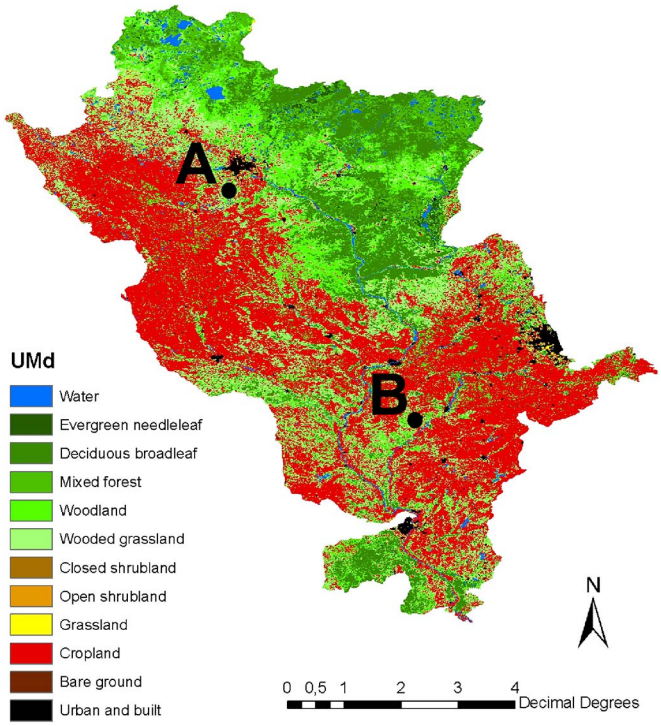

Fig. 1. Land cover map of the Upper Mississippi River Basin. The two annotated locations (A and B) will be further used in this paper as focus sites.

resulted in moderate to severe flooding, often enhanced by wet initial soil conditions. The basin is well gauged, has an extensive meteorological network, and is part of the North American Land Data Assimilation System (NLDAS) domain [31].

Fig. 1 shows two annotated areas (A and B) that correspond to the approximate locations of two SMOS grid cells, having their centers at approximately (93.45° W, 44.44° N) and (89.80° W, 40.47° N), respectively. These sites will be further used as focus sites to illustrate some of the concepts introduced in this paper. Pixel A is characterized by a clay loam soil texture and is mostly covered with low vegetation (more than 85 % of its extent) such as crops and wooded grasslands. Pixel B is located in a region consisting of a loamy soil texture and is mainly covered with high vegetation such as forests (mean fraction of forest cover $\geq$ 75 %). Therefore, both pixels have very different properties in terms of soil texture and land cover, which makes them suitable as focus sites. Moreover, due to their differences in land cover and soil texture, these sites are likely to exhibit different soil moisture states.

B. SMOS Soil Moisture Observations

The SMOS mission has been routinely providing global soil moisture data at a nominal spatial resolution of 43 km since November 2009, with a high acquisition frequency of 1 to 3 days. The SMOS soil moisture observations used in this study are level 3 CATDS (Centre Aval de Traitement des Données SMOS) data. The level 3 algorithm (i.e., version 2.4.4.) is essentially based on ESA's (European Space Agency) level 2 prototype [32], with the extension of multiorbit retrievals of vegetation parameters, enhancing the retrieval of soil moisture for individual orbits [33]. Both ascending (MIR_CLF3UA) and descending (MIR_CLF3UD) soil moisture data are available in a $\pm$25 km cylindrical projection over the Equal Area Scalable Earth grid. Data from the 1-day global product have been extracted over the Upper Mississippi area and were archived from January 15, 2010 to March 29, 2012. In addition to soil moisture, the CATDS product also includes quality indices of soil moisture and radio-frequency interference (RFI), and flags indicating the presence of snow and frozen soils. The SMOS soil moisture data have been filtered, preserving data when soil and air temperatures are larger than 2.5 °C and flags for snow and frozen soils are zero. Furthermore, only soil moisture values with a data quality index (as defined in the SMOS product) below 0.07 cm^3/cm^3 are withheld. Finally, SMOS observations, which are likely to be contaminated with RFI have been removed from the data set. Therefore, the corresponding data field (N_RFI_X and N_RFI_Y) in the SMOS product is used together with a threshold of 105 (i.e., if one of both variables, as provided with the Level 3 product, is larger than 105, the SMOS observation is not withheld).

C. VIC-Modeled Soil Moisture

The VIC model [34]–[36] is a semidistributed hydrological model, balancing both the water and energy budgets at grid sizes ranging from 1 km to hundreds of kilometers. A distinguishing characteristic of the VIC model lies in its capability to capture subgrid vegetation variability in a statistical way. VIC has been extensively used in numerous applications [37]–[40], among others.

The meteorological forcing fields used in the VIC model simulations for the Upper Mississippi basin were obtained from the real-time forcing data set [41] for the first phase of the NLDAS-1 project [31]. Seven forcing fields were processed at a 1-hourly time step and 0.125° resolution: precipitation, 2-m air temperature, atmospheric pressure, vapor pressure, wind speed, and incoming shortwave and longwave radiation. Additionally, soil and vegetation parameters were taken from the NLDAS-1 project. The land cover scheme employed in VIC is the University of Maryland 1-km global land cover data set [42], which developed based on the recommendations from the International Geosphere-Biosphere Program (IGBP) for use in global change research. Leaf area index values have been derived from AVHRR satellite observations [43]. Finally, soil texture is taken from the 1-km STATSGO database [44] and elevation data are obtained from the GTOPO30 database (30 arc seconds) [45].

VIC is run in full water and energy balance mode, to simulate soil moisture and surface temperature layers on an hourly basis, with a grid spacing of 0.125° by 0.125°. The number of vertical soil layers for moisture calculation has been set to 3, with the top layer referring to the first 10 cm. Note that the depth of this first layer arguably differs from the observation depth of SMOS (typically taken as the first 5 cm of the soil), which may be an important source of bias in soil moisture values between the observations and the model predictions of the topsoil layer. This bias may be due to the fact that observed soil moisture generally shows faster dry downs and quicker saturation [46]. Furthermore, given that the VIC model was parametrized through

optimizing for discharge predictions, it is expected that the soil moisture values may deviate from the true values in order to compensate for deficiencies in the model structure, and thus resulting in a model-specific soil moisture climatology, including an additional source of bias between observations and model simulations of soil moisture.

For this study, VIC data of the same period as that of the SMOS observations (i.e., January 15, 2010 to March 29, 2012) were used.

III. Downscaling Framework

When remotely sensed soil moisture data fields are used for updating LSMs, one is often confronted with two problems. The first stems from the difference in spatial scale, where generally the remote sensing products have a coarser resolution compared with the LSM. This problem can be solved through either upscaling the model results to the resolution of the satellite observations [30] or downscaling the coarse-scale soil moisture observations to the grid of the LSM [20], [24], [25]. The second problem concerns the fact that when the remotely sensed soil moisture observations are compared with corresponding modeled soil moisture, often a bias is encountered, which may depend on the soil moisture state. Removing this bias from the observations, such that these data are consistent with the climatology of the LSM, is currently a necessary condition for applying these observations in a data assimilation framework [47].

The framework presented in this paper is adapted from van den Berg *et al.* [48] who developed the scheme for statistically downscaling rainfall fields. For the current application, the core of the framework consists of a bivariate distribution function fitted between the coarse-scale SMOS soil moisture observations and the corresponding fine-scale modeled soil moisture values by means of a copula. Such a copula is fitted for every coarse-scale pixel in the study area. Through conditioning this distribution to a SMOS observation, the corresponding probability distribution function of VIC soil moisture values within that SMOS pixel is obtained. When this operation is performed, bias is implicitly corrected for. Yet, such a probability distribution functions does not provide a soil moisture map. In order to reach this goal, it is assumed that the spatial pattern of soil moisture values, as modeled by VIC, can be trusted, but that the soil moisture values should be adjusted according to the probability distribution function of VIC soil moisture values corresponding to the SMOS observation. Consequently, the VIC-modeled soil moisture values are adjusted through CDF-matching to this probability distribution function. In the following paragraphs, this methodology will be described in full detail.

A. Description of the Methodology

The methodology for downscaling and bias-correcting SMOS soil moisture values to the VIC resolution is based on the dependence between a SMOS coarse-scale observation, denoted by Θ_S, and the corresponding VIC top-layer soil moisture values, denoted by Θ_M, that fall within the SMOS pixel considered. To describe this dependence, a copula is used. A

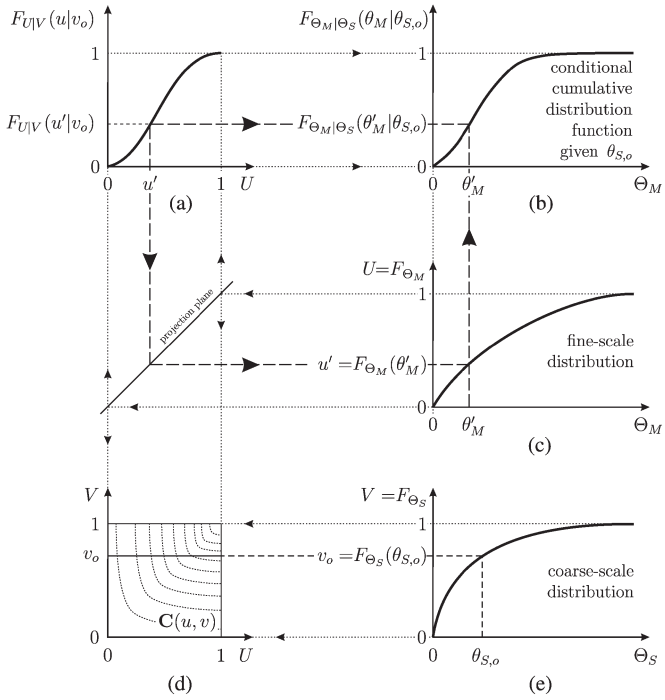

Fig. 2. Downscaling framework. The projection plane indicated in the figure allows converting values on the y-axis [in panel (c)] to x-values [in panels (a) and (d)] and *vice versa* according to $y = x$.

copula is a mathematical function that allows for constructing a multivariate distribution function based on the marginal distribution functions of the variables considered. A bivariate copula C thus models the joint cumulative probability distribution function of two random variables X and Y (in our case Θ_M and Θ_S), based on the marginal cumulative distribution functions (CDFs) $F_X(x)$ and $F_Y(y)$, as expressed by the theorem of Sklar [49]

$$\mathbb{P}(X \leq x, Y \leq y) = F_{X,Y}(x,y) = C\left(F_X(x), F_Y(y)\right) = C(u,v). \tag{1}$$

As such, the bivariate copula C corresponds to a bivariate CDF with uniform marginals U and V on the unit interval.

As the dependence between Θ_s and Θ_M may vary throughout the catchment, a copula is fitted for each coarse-scale pixel in the entire study area. Furthermore, data from different seasons, i.e., December–January–February (DJF), March–April–May (MAM), June–July–August (JJA) and September–October–November (SON), and different types of overpasses, i.e., ascending and descending, are separated. This means that for every SMOS pixel a copula is fitted for each combination of a given season and type of overpass. To fit the copulas, both VIC-modeled soil moisture values (Θ_M) and SMOS observations (Θ_S) are transformed to a uniformly distributed value on $\mathbb{I} = [0,1]$ interval, respectively, U and V, through their (marginal) cumulative distribution functions, respectively, F_{Θ_M} and F_{Θ_S} [cfr. respectively, Fig. 2(c) and (e)]. This is obtained through

$$u = F_{\Theta_M}(\theta_M) \Leftrightarrow \theta_M = F^{(-1)}_{\Theta_M}(u) \tag{2}$$

$$v = F_{\Theta_S}(\theta_S) \Leftrightarrow \theta_S = F^{(-1)}_{\Theta_S}(v) \tag{3}$$

where θ_M and θ_S are, respectively, the VIC- and SMOS-based soil moisture values, and u and v are the values of the corresponding variables U and V. $F_{\Theta_M}^{(-1)}$ and $F_{\Theta_S}^{(-1)}$ are the quasi-inverse functions of the cumulative distribution functions F_{Θ_M} and F_{Θ_S}. When these cumulative distribution functions are strictly increasing, the quasi-inverse functions equal the usual inverse F^{-1} [50].

To model the bivariate distribution function F_{Θ_M,Θ_S} between the VIC-modeled soil moisture and the coarse-scale SMOS soil moisture, the theorem of Sklar [49], (1) is used

$$F_{\Theta_M,\Theta_S}(\theta_M,\theta_S) = C\left(F_{\Theta_M}(\theta_M), F_{\Theta_S}(\theta_S)\right) = C(u,v) \quad (4)$$

where $C(u,v)$ is the copula that describes the dependence between both soil moisture variables [see Fig. 2(d)].

Based on the copula and the marginal distribution functions [see also Fig. 2(c)–(e)], the downscaling can be performed. Given a coarse-scale SMOS observation $\theta_{S,o}$, the corresponding V-value (i.e., v_o) can be found using (3). This value can then be used to condition the copula

$$F_{U|V}(u|v_o) = \mathbb{P}(U \leq u | v = v_o) = \left.\frac{\partial C(u,v)}{\partial v}\right|_{v=v_o}. \quad (5)$$

Conditioning the copula results in a conditional cumulative distribution function (CCDF) $F_{U|V}(u|v_o)$, which describes how values of u are distributed given an observation of V. This distribution function is conceptually shown in Fig. 2(a). By applying the inverse transformation in (2) and using the theorem of Sklar [see also (1)], the distribution function of corresponding θ_M-values can be derived.

To obtain the CCDF of soil moisture [cfr. Fig. 2(b)], any value $u' \in [0,1]$ [see Fig. 2(a)] is transformed to θ'_M through the inverse marginal fine-scale distribution [Fig. 2(c), i.e., $\theta'_M = F_{\Theta_M}^{[-1]}(u')$], which is subsequently assigned the value $F_{\Theta_M|\Theta_S}(\theta'_M|\theta_{S,o})$, which is equal to $F_{U|V}(u'|v_o)$. This modeled CCDF will be further referred to as $F_{\Theta_M|\Theta_S}$.

The procedure of the downscaling framework, visualized in Fig. 2, is thus applied as follows.

1) Based on the marginal CDFs of the fine-scale data F_{Θ_M} [see Fig. 2(c)] and the coarse-scale data F_{Θ_S} [given in Fig. 2(e)], that respectively allow for transforming VIC soil moisture values (θ_M) and SMOS observations θ_S into values for u and v, the copula $C(u,v)$ is fitted [see Fig. 2(d)].
2) Given a coarse-scale observation $\theta_{S,o}$, the corresponding value $v_o = F_{\Theta_S}(\theta_{S,o})$ is found [Fig. 2(e)].
3) This value v_o is used to condition the copula [Fig. 2(d)] leading to the CCDF$F_{U|V}(u|v_o)$ shown in Fig. 2(a).
4) To back-transform this CCDF to soil moisture values Θ_M, the CDF of the fine-scale distribution F_{Θ_M} [cfr. Fig. 2(c)] is inverted. As such, any value u' [as shown in Fig. 2(a)] is inverted to $\theta'_M = F_{\Theta_M}^{-1}(u')$.
5) Given the unique relationship between θ_M and u (given by F_{Θ_M}), the probability that u is smaller than or equal to any considered value u' (i.e., $\mathbb{P}(u \leq u') = F_{U|V}(u|v_o)$) is equal to the probability that θ_M is smaller than or equal to $\theta'_M = F_{\Theta_M}^{-1}(u')$. As such, the CCDF $F_{\Theta_M|\Theta_S}(\theta_M|\theta_{S,o})$ is obtained by assigning the value $F_{U|V}(u'|v_o)$ to the θ'_M corresponding to u' [cfr. Fig. 2(b)].

In order to derive downscaled soil moisture maps in accordance with the VIC climatology, two assumptions are made. First, it is assumed that the soil moisture pattern predicted by the LSM is an acceptable representation of the true soil moisture field, such that it can be imposed on the downscaled soil moisture map. The second assumption is that the downscaled soil moisture map should obey the CCDF $F_{\Theta_M|\Theta_S}$. Applying a classical CDF matching [7], [15], which transforms the CDF of the VIC-modeled soil moisture within a SMOS pixel (i.e., CCDF $F_{\Theta_M|\overline{\Theta}_M}$) to that of the derived CCDF $F_{\Theta_M|\Theta_S}$, guarantees that both assumptions are met.

In the current setup of the experiment, the number of fine-scale VIC pixels within the overlaying coarse-scale SMOS pixel is too small (i.e., 4 to 6) to derive an empirical VIC soil moisture distribution function. Using the ranks to estimate the cumulative distribution value is too inaccurate, and an alternative estimation approach is needed to estimate the distribution function of modeled soil moisture values of the individual VIC grid cells within the SMOS pixel. Experiments have shown that the spatial variability of soil moisture depends on the spatial average soil moisture content [51], thus requiring probability distribution functions that change with the average moisture content. One way to represent the required distribution function of the modeled soil moisture is by accounting for the (fitted) scaling relationship between the standard deviation of the soil moisture content values within the area considered and the corresponding averaged value, and assuming a known distribution function such as a Gaussian probability distribution function for the fine-scale soil moisture values, as done by Vernieuwe *et al.* [52]. However, to avoid predefining the type of distribution function, another approach that is consistent with the downscaling methodology is used.

To properly describe the within SMOS-pixel soil moisture distribution function, a methodology that makes use of the same scaling framework as previously presented is suggested that allows for a proper CDF-matching. Through constructing a copula between data couples $(\theta_M, \overline{\theta}_M)$, where $\overline{\theta}_M$ is the mean modeled soil moisture within the SMOS pixel, the required CCDF $F_{\Theta_M|\overline{\Theta}_M}$ can be obtained through conditioning this copula on the average soil moisture content, modeled at the time of SMOS acquisition. The rationale for this approach is the relationship between the average soil moisture content and the distribution of the soil moisture values at the model scale within a SMOS pixel. To obtain this CCDF, the framework discussed above can be followed by considering $\overline{\Theta}_V$ instead of Θ_S. As a result the CCDF $F_{\Theta_M|\overline{\Theta}_M}$ is obtained, which can be used to calculate the cumulative distribution value of the soil moisture content for each of the VIC pixels.

Once the cumulative distribution values of the individual VIC pixels are known, a CDF matching can be performed, which transforms $F_{\Theta_M|\overline{\Theta}_M}$ to $F_{\Theta_M|\Theta_S}$. This is obtained through altering the soil moisture value of the modeled VIC pixel to the value that has the same cumulative distribution value in $F_{\Theta_M|\Theta_S}$, i.e., a CDF matching between $F_{\Theta_M|\overline{\Theta}_M}$ and $F_{\Theta_M|\Theta_S}$.

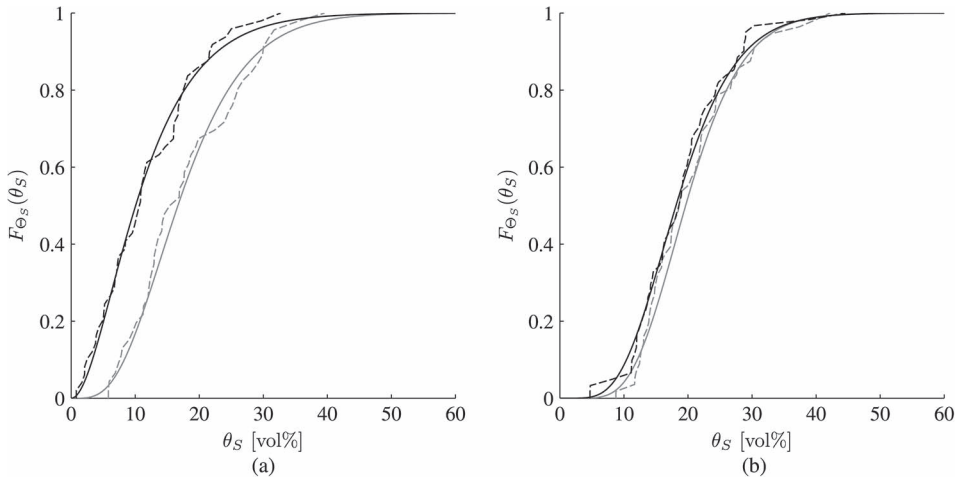

Fig. 3. Marginal distribution functions for the ascending (a) and descending (b) SMOS data in set S_1 for pixels A (black lines) and B (gray lines) for the third season (JJA). Empirical distribution functions are plotted as dotted lines and the theoretical models fitted to the data are shown as solid lines.

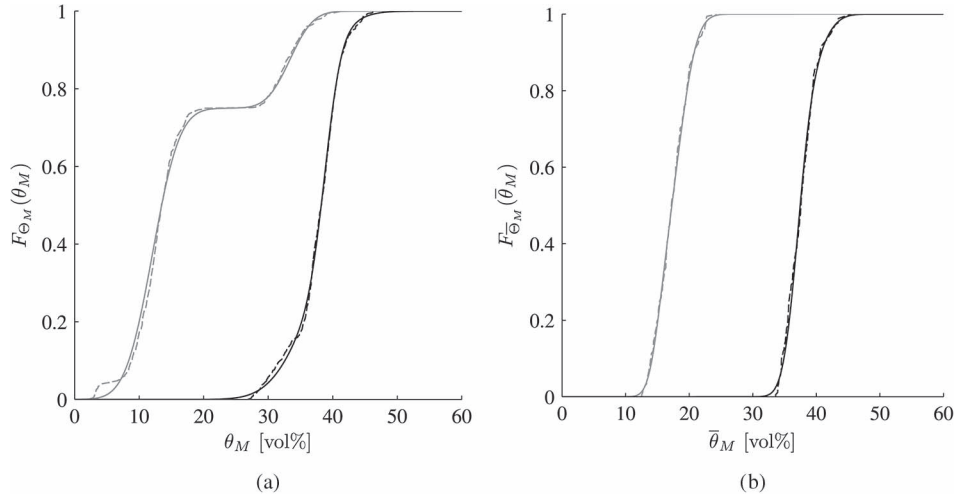

Fig. 4. Marginal distribution functions for the VIC-modeled fine-scale (a) and coarse-scale (b) soil moisture values in set S_1 for pixels A (black lines) and B (gray lines) for the third season (JJA). Empirical distribution functions are plotted as dotted lines and the theoretical models fitted to the data are shown as solid lines.

B. Fitting the Marginal Distribution Functions

Three marginal cumulative distribution functions are needed to perform the downscaling, i.e., $F_{\Theta_S}(\theta_S)$, $F_{\Theta_M}(\theta_M)$, and $F_{\overline{\Theta}_M}(\overline{\theta}_M)$. However, as the ascending and descending SMOS data sets are treated separately, each coarse-scale pixel considered in this study requires four marginal distribution functions that need to be derived for each season. To maintain the practical applicability of the downscaling framework, marginal distribution functions are fitted to the empirical cumulative distribution values. It should be noted that distribution functions are only fitted if at least 100 data points are available. Several parametrical distributions were considered and the distribution functions used were selected based on a visual and statistical inspection of the different fits. Based on this inspection, the Gamma distribution was selected to model the statistical behavior of both the ascending and descending SMOS soil moisture. In contrast, the Gaussian Mixture distribution with two components was used to model the bimodal distribution function that is often encountered for the modeled VIC soil moisture (for $F_{\Theta_M}(\theta_M)$ as well as $F_{\overline{\Theta}_M}(\overline{\theta}_M)$). The parameters of the different distribution functions were obtained using a classical maximum likelihood estimation. However, one should be aware that for some pixels another theoretical distribution function may better fit the data. However, it was decided to select only one model for each type of fit, to safeguard the operational applicability of the framework.

Figs. 3 and 4 show the fitted marginal distribution functions (solid lines) and the empirical marginal distribution functions (dotted lines) for the two coarse-scale pixels A and B (cf. Fig. 1). These figures show the models fitted to the data in S_1 and for the third season (JJA) considered in this study. For the other seasons and for the other data set S_2, similar results were obtained (figures not shown). Given the relatively good agreement between the theoretical models and the empirical distribution functions, it can be concluded that the selected models are suitable to describe the statistics of the different soil moisture products.

Figs. 3 and 4 also show that an important difference may exist between the distributions of the different coarse-scale pixels. This is due to several influencing factors such as soil texture,

land cover, topography, homogeneity of the coarse-scale pixel, etc., and motivates the choice to fit the different models for each of the pixels separately.

Comparing Fig. 3(a) and (b) reveals that there is a difference between the marginal cumulative distribution function fitted to the ascending SMOS soil moisture data and the one fitted to the descending SMOS soil moisture data, which shows the need to treat them separately. This difference in statistical behavior between the ascending SMOS soil moisture products and the descending SMOS soil moisture products may be attributed to several factors. It is well known that the atmospheric and environmental conditions during both acquisitions differ rather strongly. During the ascending overpass (6 am local solar time) ionospheric effects are generally lower compared with the descending overpass (6 pm local solar time). Moreover, the physical temperatures of the soil and vegetation layers can be considered more in equilibrium during the ascending overpass of the satellite. Furthermore, RFI impacts are different between ascending and descending passes, and although the data are filtered for RFI, its effects are never completely removed. These differences influence the soil moisture retrieval, which may result in a different cumulative distribution function for both data sets. This significant deviation between the two types of overpasses could not be observed for the corresponding VIC distributions. Therefore, only one distribution function was fitted to the modeled soil moisture values from VIC.

Fig. 4(a) clearly illustrates why a Gaussian mixture distribution function is selected to model the marginal cumulative distribution function of the fine-scale VIC soil moisture. It is shown that the distribution function of pixel B consists of two components, whereas this behavior is not observed for pixel A. However, the Gaussian mixture model seems sufficiently flexible to model the empirical distribution function of the latter pixel as well. While alternative distributions that better fit the distribution at every pixel may exist (more dedicated research could find the best fitting function per pixel), distributions functions with a flexible shape were used, as they are easy to parameterize and are the same for each pixel (though differing in parameter values).

The shape of the marginal cumulative distribution functions considered in Fig. 4(a) are strongly driven by the soil properties. Homogeneous pixels in terms of soil properties are more likely to have a low variability of soil moisture within the pixel, which results in a cumulative distribution function like the one of pixel A, as shown in Fig. 4(a). When soil properties are non-uniform in the area considered, the soil moisture variability is likely to increase. This is the case for pixel B, where the soil textural properties of one fine-scale VIC pixel located within the SMOS pixel, strongly deviate from the other VIC pixels located within the same SMOS pixel. On average, this pixel exhibits higher soil moisture states compared with the others, resulting in a bimodal probability distribution function.

Figs. 3 and 4(b) further show that there is a bias between the aggregated VIC and SMOS soil moisture. In addition, the dynamic range of the VIC top-layer soil moisture values is generally lower than the one observed for the SMOS soil moisture data set. It will be shown that the framework presented in this paper implicitly accounts for this bias.

TABLE I
SELECTED COPULA FAMILIES AND CORRESPONDING PARAMETERS VALUES FOR JJA FOR PIXELS A AND B

	Pixel A		**Pixel B**	
	Family	α	*Family*	α
SMOS coarse - VIC fine (Asc.)	Frank	3.45	Frank	3.09
SMOS coarse - VIC fine (Desc.)	Frank	1.93	Frank	1.03
VIC fine - VIC coarse	Gumbel	2.69	Frank	4.66

C. Fitting the Copulas

Aside from the marginal cumulative distribution functions, three copulas are needed for each pixel in order to apply the downscaling framework: two copulas describing the dependences between the VIC fine-scale soil moisture and the SMOS coarse-scale soil moisture (i.e., one for ascending and one for descending overpasses) and one copula describing the relation between aggregated VIC soil moisture values and the corresponding fine-scale VIC-modeled soil moisture values. Both non-parametric empirical copulas and theoretical parametric copulas can be used to describe the dependence structure between two variables. Given the objective to apply the framework in an operational application, parametric copulas are preferred as these allow for a fast calculation of the CCDF. Although more suitable copulas can probably be found, we restricted the search for the best parametric copula to the three most widely used families of Archimedean copulas [53]. It is believed that these families are sufficiently flexible to describe the dependence structures found in the data sets. The following families are included in the analysis:

- the Frank copula family

$$C(u,v) = -\frac{1}{\alpha}\ln\left(1 + \frac{(e^{-\alpha u}-1)(e^{-\alpha v}-1)}{e^{-\alpha}-1}\right) \quad (6)$$

  with $\alpha \in]-\infty, +\infty[\backslash\{0\}$;
- the Gumbel copula family

$$C(u,v) = \exp\left(-\left[(-\ln(u))^{\alpha} + (-\ln(v))^{\alpha}\right]^{\frac{1}{\alpha}}\right) \quad (7)$$

  with $\alpha \in [1, +\infty[$;
- the Clayton copula family

$$C(u,v) = \max\left(\left[u^{-\alpha} + v^{-\alpha} - 1\right]^{-\frac{1}{\alpha}}, 0\right) \quad (8)$$

  with $\alpha \in [-1, +\infty[\backslash\{0\}$.

An additional advantage of these copula families is that only one parameter (α) has to be estimated.

Most commonly, the best copula is selected based on a likelihood approach or goodness-of-fit test for copulas (e.g., [54] and [55]). However, these tests only allow for parameterized copulas to be compared [56]. To select the most suitable copula family, an alternative technique is needed that is independent of the copula parameters. Therefore, the recently developed Bayesian copula selection algorithm [56] was applied. It should be emphasized here that a restricted set of copula families is selected *a priori* in this study [see also (6)–(8)]. Once the most appropriate copula family is selected, the parameter α of each copula is calculated by using the relationship between Kendall's

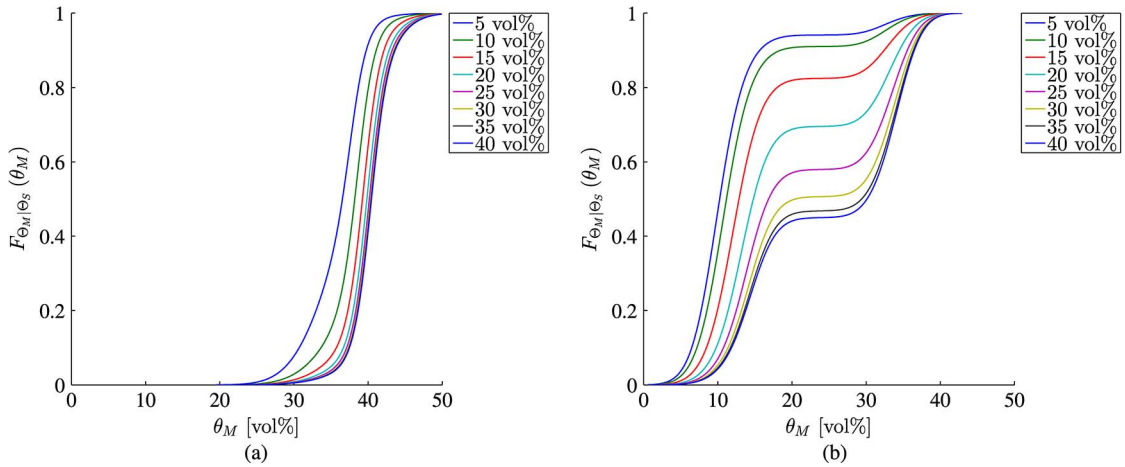

Fig. 5. CCDF $F_{\Theta_M|\Theta_S}$ for different values of the coarse-scale SMOS observation for pixel A (a) or pixel B (b) for the ascending data set and the third season (JJA) considered.

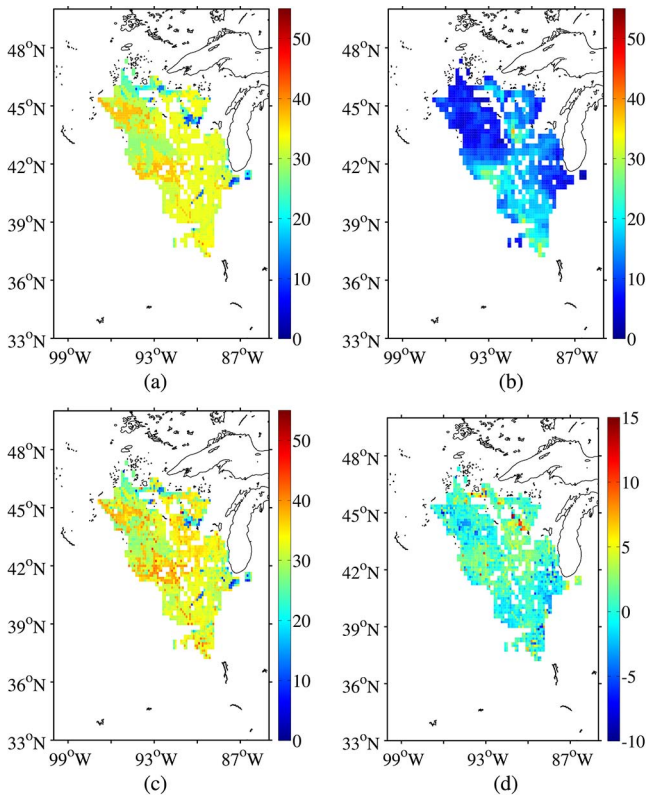

Fig. 6. (a) VIC simulation on 17/08/2010 at 6 AM local solar time (during the ascending SMOS overpass), (b) corresponding ascending SMOS observations, (c) downscaled soil moisture map and (d) difference map, i.e., panel (c) minus panel (a). All soil moisture contents are expressed as vol%.

tau (τ) and the copula parameter. The relationships between τ and α for the Frank, Gumbel and Clayton copula families are respectively given by

$$\tau = 1 - \frac{4}{\alpha}\left(1 - \frac{1}{\alpha}\int_0^{\alpha} \frac{t}{\exp(t) - 1} dt\right) \tag{9}$$

$$\tau = 1 - \alpha^{-1} \tag{10}$$

$$\tau = 1 - \frac{2}{2 + \alpha}. \tag{11}$$

The selected copula families are listed in Table I.

D. CDF of Downscaled Soil Moisture

The cumulative distribution function of the downscaled SMOS soil moisture is obtained through conditioning the copula to the SMOS observation, resulting in the CCDF $F_{\Theta_M|\Theta_S}$. This CCDF is obtained through a numerical approximation of (5)

$$F_{U|V}(u, v_o) = \left.\frac{\partial C(u, v)}{\partial v}\right|_{v=v_o} \approx \frac{C(u, v_o + \delta) - C(u, v_o)}{\delta}. \tag{12}$$

A value of $\delta = 1 \cdot 10^{-5}$ is selected to approximate the derivatives, whereas U is linearly discretized between 0 and 1 with a step size of $1 \cdot 10^{-2}$. The resulting distribution function $F_{U|V}$ can be transformed to $F_{\Theta_M|\Theta_S}$ by using the inverse transformation in (2) and the theorem of Sklar.

Fig. 5 shows the resulting CCDF $F_{\Theta_M|\Theta_S}$ for a variety of possible SMOS observations for the third season and the ascending data set for pixels A and B, respectively. Both plots in this figure clearly show that the conditional distribution of the fine-scale soil moisture deviates from the distribution of the corresponding coarse-scale soil moisture values [see also Fig. 3(a)]. However, the shape of the CCDFs is very similar to the shape of the distribution of the corresponding fine-scale VIC soil moisture values [see also Fig. 4(a)]. This can be expected given the objective of the framework was to estimate the distribution of the subpixel soil moisture values given a coarse-scale SMOS observation. This indicates that the fitted copulas are able to model the distribution of the fine-scale soil moisture values. Moreover, as could be expected, the CCDFs of different pixels can be very different, as already discussed.

Both figures also show that depending on the coarse-scale SMOS observation, different CCDFs are obtained. For instance, Fig. 5(a) shows that the expected fine-scale soil moisture variability is decreasing when the observed SMOS soil moisture value is increasing. Alternatively, Fig. 5(b) shows that for increasing values of the coarse-scale soil moisture observation, it is more likely to observe a multimodal fine-scale soil moisture distribution function.

IV. Results

The objective of the downscaling framework is to rescale the SMOS observations to the VIC resolution and to remove the bias between both soil moisture products. The resulting soil moisture product should thus obey the VIC climatology. This means that the downscaled soil moisture map should reflect the spatial soil moisture pattern predicted by VIC, but rescaled to the distribution of fine-scale soil moisture values given a coarse-scale SMOS observation. To assess the ability of the framework to meet these objectives, the SMOS observations in data set S_2 are downscaled using the copulas fitted to data from S_1.

A. Downscaled Soil Moisture Maps

Fig. 6 shows an example of the VIC simulations, the ascending coarse-scale SMOS observations, the corresponding downscaled SMOS observations on August 17, 2010, as well as a difference image of the VIC simulations with the downscaled SMOS observations. Locations where no soil moisture value is shown correspond to pixels where either no SMOS observation is available or where no copula could be fitted due to the low data availability.

Comparing Fig. 6(a) and (b), it is clear that the modeled soil moisture exceeds the observed soil moisture by SMOS on average. However, the spatial patterns of both products are comparable for a large part of the study area. Fig. 6(c) shows the corresponding downscaled product. As shown from this figure, the downscaled product reflects the soil moisture patterns predicted by VIC. Furthermore, it can be seen that the soil moisture value at several zones in the study area is increased compared with the original VIC product [cf. Fig. 6(d)], and that the fine-scale variability at several locations is slightly increased. This means that, on average, a higher variability of the fine-scale soil moisture observations is expected than what is predicted by VIC for some of the SMOS observations. Figs. 7 and 8 demonstrate this with an example of one coarse-scale SMOS observation. Fig. 7 shows the marginal cumulative distribution function of fine-scale soil moisture at pixel A given a coarse-scale SMOS observation ($F_{\Theta_M|\Theta_S}$, red line) and the cumulative distribution function of modeled soil moisture, given its average value at the coarse scale (i.e., CCDF $F_{\Theta_M|\overline{\Theta}_M}$, black line). Both marginal distribution functions stem from conditioning the respective copulas with a coarse-scale SMOS observation and a mean modeled soil moisture value, respectively. As shown from this figure, a slight discrepancy between both marginal distribution functions can be observed, indicating that the CDF matching will result in slightly rescaled soil moisture values. This is illustrated in Fig. 8 where the modeled VIC soil moisture values, at pixel A, are shown in the left panel and the corresponding downscaled SMOS observations are shown in the right panel. As shown from the left panel of this figure, all modeled soil moisture values are restricted between 4 and 33 vol%. It is clear from Fig. 7 that higher soil moisture values are expected. After CDF matching, higher soil moisture values will thus be obtained, which is shown at the right-hand side of Fig. 8. Furthermore, the range of soil moisture values is slightly increased, resulting in a higher fine-scale soil moisture variability as already observed at certain locations in Fig. 6.

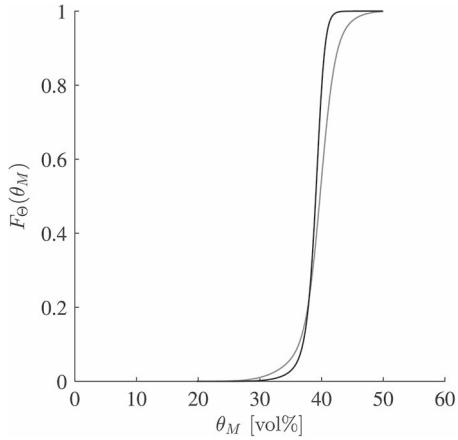

Fig. 7. $F_{\Theta_M|\Theta_S}$ (gray line) and $F_{\Theta_M|\overline{\Theta}_M}$ (black line) on 17/08/2010 for pixel A (ascending SMOS overpass).

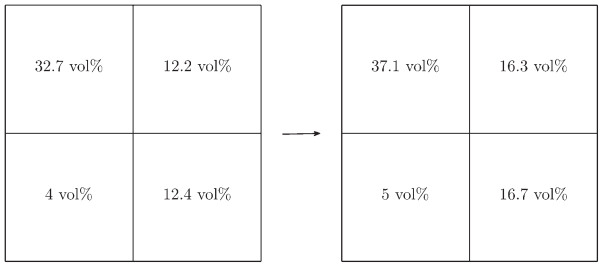

Fig. 8. VIC simulations (left-hand side) and corresponding downscaled SMOS soil moisture (right-hand side) on 17/08/2010 for pixel A (ascending SMOS overpass). All soil moisture contents are expressed as vol%.

Fig. 9 shows another example of a VIC simulation, the corresponding ascending SMOS observations and the downscaled soil moisture map, respectively, for April 18, 2011, with the soil moisture patterns modeled by VIC deviating strongly from the observed soil moisture patterns by SMOS. This is particularly true for the high soil moisture zone predicted by VIC in the central part of the study area. It is clear from Fig. 9(b) that SMOS observes a zone with low soil moisture compared with its surroundings. Fig. 9(c) shows again that the resulting downscaled product reflects the soil moisture patterns predicted by VIC. It can be seen that the soil moisture values at the central part of the study area are reduced compared with the original VIC simulations [cfr. Fig. 9(d)]. This means that, on average, and given the SMOS observations in this zone, lower soil moisture values are expected than the ones modeled by VIC.

The results presented here show the flexibility of the downscaling framework. It is shown that the SMOS observations are the key variables to estimate how fine-scale soil moisture values are distributed given a coarse-scale soil moisture observation. The CDF matching between the distribution function $F_{\Theta_M|\Theta_S}$ and the observed cumulative distribution function $F_{\Theta_M|\overline{\Theta}_M}$ guarantees that the downscaled soil moisture values are distributed as would be expected, which will benefit the data assimilation since the downscaled product will obey the VIC climatology.

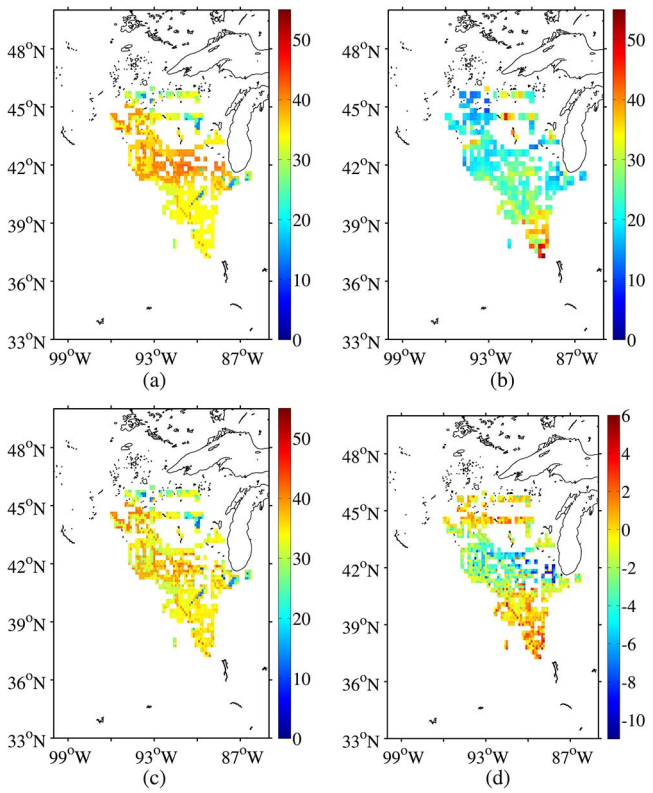

Fig. 9. (a) VIC simulation on 18/04/2011 at 6 AM local solar time (during the ascending SMOS overpass), (b) corresponding ascending SMOS observations, (c) downscaled soil moisture map and (d) difference map, i.e., panel (c) minus panel (a). All soil moisture contents are expressed as vol%.

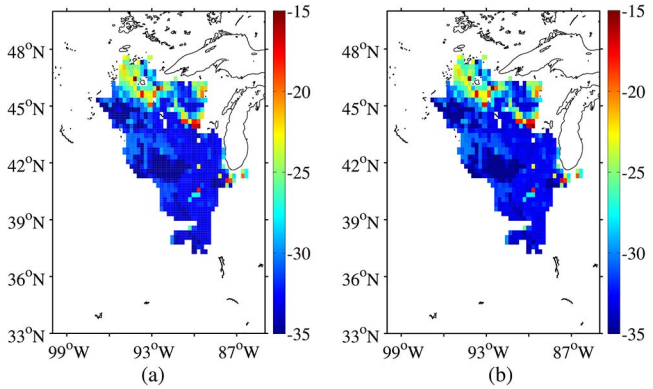

Fig. 10. Temporal bias before downscaling for the ascending (a) and descending (b) data set, expressed in vol%.

B. Bias

Prior to the assimilation of satellite-derived soil moisture products into LSMs, the bias between the simulated and observed soil moisture products should be removed [10]. The downscaling framework presented in this paper implicitly removes the bias between both products. To verify this, the temporal bias between the SMOS observations and the simulated VIC soil moisture values was calculated on a pixel basis for the entire S_2 data set.

Fig. 10 shows maps of the bias between the observed coarse-scale SMOS observations and the simulated VIC soil moisture values for the ascending and descending tracks, respectively. To obtain this, the modeled VIC soil moisture was aggregated

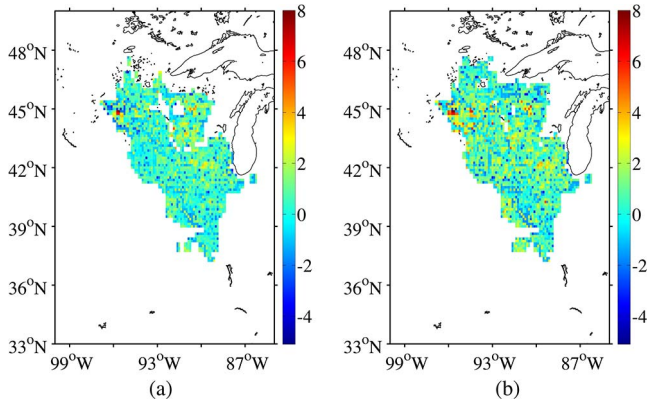

Fig. 11. Temporal bias after downscaling for the ascending (a) and descending (b) data set, expressed in vol%.

to the SMOS scale by simply averaging the VIC simulations located within a given SMOS pixel. As can be seen from these figures, a negative bias exists between both soil moisture products. This indicates that, on average, the observed SMOS soil moisture is smaller compared with the modeled soil moisture values by VIC. This bias can also be observed when the cumulative distribution functions of both products are compared [see also Figs. 3 and 4(b)]. The figures also show a lower bias (in absolute terms) for the northern part compared with the remainder of the study area. However, it should be noted that the northern part is dominated by forests (cfr. Fig. 1) and that the data availability for these areas is somewhat lower. Furthermore, no clear difference in bias can be observed for both types of overpasses.

Fig. 11 displays the bias after downscaling, based on the framework for which the copulas were fitted to data in S_1. It is clear from this figure that the bias between the original SMOS soil moisture map and the VIC simulation is strongly reduced. Unfortunately, some pixels can still be found with a high temporal bias. However, more than 95 % of the pixels have an absolute bias below 3 vol% for both the ascending and descending overpasses, indicating that the framework is able to remove the bias from the observations under most circumstances. It is also clear from Fig. 11 that no spatial pattern can be observed in the bias. The difference in bias between the ascending and descending track is slightly more distinct compared with the bias before downscaling, with a slightly higher bias for the descending data set.

C. Robustness of the Framework

Given the objective to develop a framework that can be implemented operationally, the question arises whether the fitted copulas are robust. It should be emphasized that the calibration data set should be sufficiently large such that all possible soil moisture states are included in the analysis, as a copula fitted to a rather wet year, will not perform as expected when applied on a rather dry year. To circumvent this problem, the data set in this study was randomly split into two parts (i.e., S_1 and S_2), rather than splitting the data into two separate years, as this may lead to applying the framework in situations that were not (or insufficiently) covered in the calibration period (cfr. supra).

To assess the robustness of the framework, the marginal distribution functions and copulas were fitted for each pixel

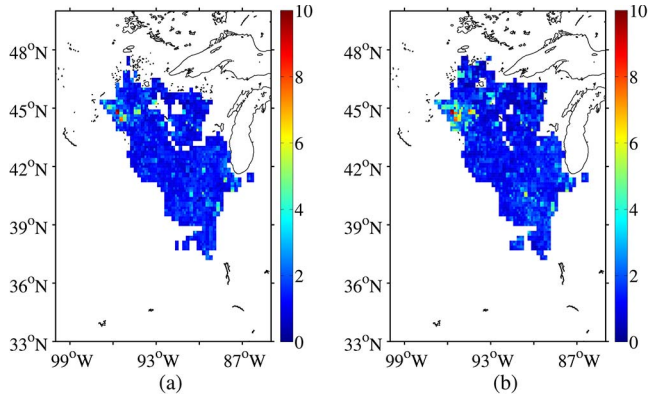

Fig. 12. Root Mean Squared Error (vol%) between the downscaled SMOS data obtained through the downscaling framework with copulas fitted to S_1 on the one hand and fitted to S_2 on the other hand, for ascending (a) and descending (b) observations.

separately, once to the data from S_1 and once to data from S_2. For both data sets, marginal cumulative distribution functions and copulas for each coarse-scale pixel in the entire study area and for each season and type of overpass are thus obtained. Subsequently, each SMOS data set was downscaled using both parameter sets. Finally, the downscaled soil moisture maps were compared with assess whether both parameter sets gave rise to the same results.

Fig. 12 shows maps of the root-mean-squared error (RMSE) calculated between downscaled SMOS observations using the framework for which the copulas were fitted to S_1 and those downscaled with the framework having copulas fitted to S_2, distinguishing between the ascending and descending tracks. From these figures it can be seen that for both types of overpasses, the models (i.e., marginal distributions and copulas) are robust for most of the pixels, based on the small values of the RMSE for the majority of the study area. This means that downscaling the SMOS observations with both parameter sets gave rise to the same results. Therefore, it can be expected that the fitted models are stable in time. Fig. 12 also demonstrates that there is a small problematic zone in the north western part of the study area where the values of the RMSE are somewhat higher compared with the remaining pixels in the study site. When Fig. 11 is compared with Fig. 12, it can be seen that the pixels, where an elevated bias is observed, are the same pixels where the temporal stability of the models is weak. This can probably be attributed to a combination of data availability and the complexity of the dependence between the different variables in this zone. As aforementioned, a threshold of 100 data points was defined to fit the different models. However, this threshold was determined in a subjective way and can be adapted in the future to optimize the fits.

D. Time Series of Downscaled Soil Moisture

As an example, Fig. 13 plots time series of soil moisture for a fine-scale VIC pixel at location A and another at location B for the third season of the year 2010, along with the observed coarse-scale SMOS soil moisture and the downscaled soil moisture value for the fine-scale pixel considered. The downscaled soil moisture values shown in these plots are obtained from

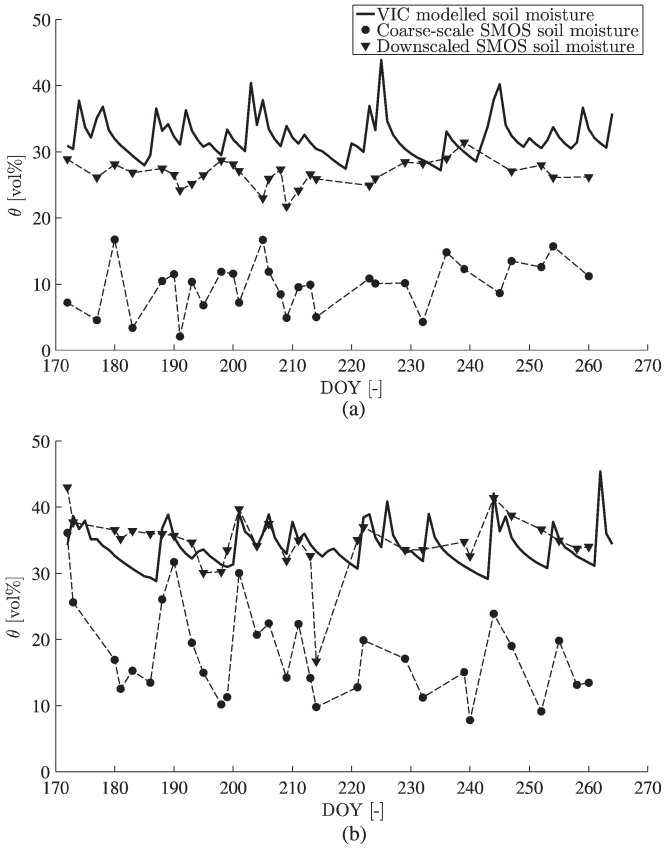

Fig. 13. Time series of soil moisture for one random fine-scale VIC pixel located within the coarse-scale SMOS pixel A (a) and pixel B (b) for the third season (JJA) of the year 2010 (black line), and corresponding SMOS coarse-scale and downscaled soil moisture values.

the independent SMOS data sets. Both figures again show the large bias between the coarse-scale SMOS observations and the VIC simulations. Further, both figures clearly demonstrate that there is a strong difference between the original CATDS Level-3 SMOS soil moisture values and those obtained after downscaling.

Fig. 13(a) shows that, on average, the downscaled soil moisture values are lower than the VIC simulations. This indicates that lower VIC soil moisture values are expected based on the SMOS observations. Yet, the behavior of the downscaled soil moisture is dictated by both the SMOS observation and the fine-scale VIC simulations located in the coarse-scale pixel. For pixel B, the differences between the downscaled soil moisture and the VIC simulations is less pronounced [see Fig. 13(b)]. Only at some specific time steps is a large difference obtained, whereas for most of the time steps the downscaled soil moisture corresponds well to the VIC simulations. The reason for the large differences have to be investigated in further detail, as these can be attributed to errors in model forcing and an insufficient fit of copulas or marginal distribution functions in certain ranges of observed and/or simulated soil moisture, etc.

V. Conclusion

A statistical framework has been proposed to downscale remotely sensed coarse-scale soil moisture observations for the purpose of assimilating into a higher resolution LSM. Given the

potential difference in climatology of the model with respect to the remotely sensed observations, a bias may exist between the two products. Yet, such a bias needs to be removed when assimilating the observations. To reach both goals, i.e., a spatial downscaling and bias removal, a downscaling framework that makes use of a copula has been proposed. Through conditioning the copula to the coarse-scale observation, the subgrid variability of the LSM-based soil moisture is modeled through the CCDF of downscaled soil moisture values. In order to preserve the spatial pattern within the SMOS pixel, a CDF matching procedure is applied, in which the modeled soil moisture was rescaled to this CCDF.

The advantage of the proposed methodology is that it can be applied irrespective of boundary conditions (i.e., it is not restricted to semiarid or humid catchments, e.g., [24]), LSM or remote sensing product used, as it merely depends on the statistical dependence between two data sets (i.e., remotely sensed and modeled soil moisture). In this paper, the method is demonstrated using SMOS-based soil moisture and the VIC model for the Upper Mississippi Basin. It is shown that the method allows the downscaling of SMOS products to the VIC resolution while adequately removing the bias. However, further research is needed with respect to optimizing the fits of the marginal distribution functions. In this paper, flexible distribution functions were used allowing for modeling bimodal distributions. However, other probability distribution functions may be found that better represent the data. Further, the copulas used were restricted to three flexible and commonly used copula families that are easily parameterized based on one single parameter. Again, alternative models can be proposed that better describe the dependences. Finally, the minimal number of data points needed to fit the copulas was set to 100. This value allowed for most of the pixels to be parameterized, but it should be investigated whether this lower limit with respect to the number of data points could be increased, if more data were available. Notwithstanding these comments, it was found that the approach is very robust, and that copulas fitted to model predictions can be used to downscale SMOS observations at dates not included in the calibration data set. However, when the framework is to be applied in an operational setting, it is best to fit the copulas to the maximum extent of data available, i.e., all historical data available, in order to prevent that the framework is applied outside its validity (as defined by the data used for fitting the copulas in the framework). Furthermore, a regular refitting of the copulas with newly available data while time is progressing is advisable, to ensure that the data set used for calibration is as rich as possible, reflecting the soil moisture climatologies as accurate as possible given the data set.

It should be remarked that the presented framework only provides soil moisture maps at the resolution of the hydrological model. In order to use these maps for data assimilation, an assessment of the uncertainty on each of the subgrid soil moisture values should be made based on the uncertainty of the SMOS observation. Latter downscaling of the uncertainty is currently under investigation.

Finally, it should be clear that the methodology developed can be used for other purposes than data assimilation. It allows for downscaling coarse-scale data (not restricted to soil moisture) to a higher resolution at which data, being modeled or remotely sensed, are available. Further research should be undertaken to assess whether both data sources need to represent the same state variable, or whether both can be different though related to each other (e.g., brightness temperature and soil moisture).

REFERENCES

[1] S. A. Margulis, D. McLaughlin, D. Entekhabi, and S. Dunne, "Land data assimilation and estimation of soil moisture using measurements from the Southern Great Plains 1997 Field Experiment," *Water Resour. Res.*, vol. 38, no. 12, pp. 35-1–35-18, Dec. 2002.

[2] W. T. Crow and E. F. Wood, "The assimilation of remotely sensed soil brightness temperature imagery into a land surface model using ensemble Kalman filtering: A case study based on ESTAR measurements during SGP97," *Adv. Water Resour.*, vol. 26, no. 2, pp. 137–149, Feb. 2003.

[3] R. Reichle *et al.*, "Comparison and assimilation of global soil moisture retrievals from the Advanced Microwave Scanning Radiometer for the Earth Observing System (AMSR-E) and the Scanning Multichannel Microwave Radiometer (SMMR)," *J. Geophys. Res.*, vol. 112, no. D9, pp. D09108-1–D09108-14, May 2007.

[4] V. R. N. Pauwels, R. Hoeben, N. E. C. Verhoest, and F. P. De Troch, "The importance of the spatial patterns of remotely sensed soil moisture in the improvement of discharge predictions for small-scale basins through data assimilation," *J. Hydrol.*, vol. 251, no. 1–2, pp. 88–102, Sep. 2001.

[5] V. R. N. Pauwels, R. Hoeben, N. E. C. Verhoest, F. P. De Troch, and P. A. Troch, "Improvement of TOPLATS-based discharge predictions through assimilation of ERS-based remotely sensed soil moisture values," *Hydrol. Proc.*, vol. 16, no. 5, pp. 995–1013, Apr. 2002.

[6] R. Reichle, R. D. Koster, J. Dong, and A. Berg, "Global soil moisture from satellite observations, land surface models, and ground data: Implications for data assimilation," *J. Hydrometeor.*, vol. 5, no. 3, pp. 430–442, Jun. 2004.

[7] M. Drusch, E. F. Wood, and H. Gao, "Observation operators for the direct assimilation of TRMM microwave imager retrieved soil moisture," *Geophys. Res. Lett.*, vol. 32, no. 15, p. L15403, 2005.

[8] H. Gao, T. J. Jackson, M. Drusch, and R. Bindlish, "Using TRMM/TMI to retrieve surface soil moisture over the southern United States from 1998 to 2002," *J. Hydrometeor.*, vol. 7, no. 1, pp. 23–38, Feb. 2006.

[9] A. K. Sahoo, G. J. M. De Lannoy, R. H. Reichle, and P. R. Houser, "Assimilation and downscaling of satellite observed soil moisture over the Little River Experimental Watershed in Georgia, USA," *Adv. Water Res.*, vol. 52, pp. 19–33, Feb. 2013.

[10] G. J. M. De Lannoy, P. R. Houser, V. R. N. Pauwels, and N. E. C. Verhoest, "State and bias estimation for soil moisture profiles by an ensemble Kalman filter," *Water Resour. Res.*, vol. 43, no. 6, pp. W06401-1–W06401-15, Jun. 2007.

[11] M. Pan, A. K. Sahoo, and E. F. Wood, "Improving global soil moisture retrievals from a physically based radiative transfer model," *Remote Sens. Environ.*, vol. 140, pp. 130–140, 2014.

[12] H. Wilker, M. Drusch, G. Seuffert, and C. Simmer, "Effects of the near-surface soil moisture profile on the assimilation of L-band microwave brightness temperature," *J. Hydrometeor.*, vol. 7, no. 3, pp. 433–442, Jun. 2006.

[13] R. D. Koster *et al.*, "On the nature of soil moisture in land surface models," *J. Climate*, vol. 22, no. 16, pp. 4322–4335, Aug. 2009.

[14] R. Reichle and R. D. Koster, "Bias reduction in short records of satellite soil moisture," *Geophys. Res. Lett.*, vol. 31, no. 19, p. L19501, Oct. 2004.

[15] R. Reichle and R. D. Koster, "Global assimilation of satellite surface soil moisture retrievals into the NASA Catchment Land Surface Model," *Geophys. Res. Lett.*, vol. 32, no. 2, pp. L02404-1–L02404-4, Jan. 2005.

[16] W. Ni-Meister, J. Walker, and P. R. Houser, "Soil moisture initialization for climate prediction: Characterization of model and observation errors," *J. Geophys. Res.*, vol. 110, no. D13, pp. D13111-1–D13111-14, Jul. 2005.

[17] A. K. Griffith and N. K. Nichols, "Adjoint techniques in data assimilation for estimating model error," *J. Flow, Turbulence Combustion*, vol. 65, no. 3/4, pp. 469–488, 2000.

[18] R. Reichle, D. B. McLaughlin, and D. Entekhabi, "Hydrologic data assimilation with the ensemble Kalman filter," *Mon. Weather Rev.*, vol. 130, no. 1, pp. 103–114, Jan. 2002.

[19] D. Ryu, W. T. Crow, X. Zhan, and T. J. Jackson, "Correcting unintended perturbation biases in hydrologic data assimilation," *J. Hydrometeor.*, vol. 10, no. 3, pp. 734–750, Jun. 2009.
[20] Y. H. Kaheil, M. K. Gill, M. McKee, L. A. Bastidas, and E. Rosero, "Downscaling and assimilation of surface soil moisture using ground truth measurements," *IEEE Trans. Geosci. Remote Sens.*, vol. 46, no. 5, pp. 1375–1384, May 2008.
[21] T. Kawanishi *et al.*, "The Advanced Microwave Scanning Radiometer for the Earth Observing System (AMSR-E), NASDA's contribution to the EOS for global energy and water cycle studies," *IEEE Trans. Geosci. Remote Sens.*, vol. 41, no. 2, pp. 184–194, Feb. 2003.
[22] Y. H. Kerr *et al.*, "Soil moisture retrieval from space: The Soil Moisture and Ocean Salinity (SMOS) mission," *IEEE Trans. Geosci. Remote Sens.*, vol. 39, no. 8, pp. 1729–1735, Aug. 2001.
[23] D. Entekhabi *et al.*, "The Soil Moisture Active Passive (SMAP) mission," *Proc. IEEE*, vol. 98, no. 5, pp. 704–716, May 2010.
[24] O. Merlin, A. Chehbouni, G. Boulet, and Y. H. Kerr, "Assimilation of disaggregated microwave soil moisture into a hydrologic model using coarse-scale meteorological data," *J. Hydrometeor.*, vol. 7, no. 6, pp. 1308–1322, Dec. 2006.
[25] L. M. Parada and X. Liang, "A downscaling framework for L band radio brightness temperature imagery," *J. Geophys. Res.*, vol. 108, no. D22, p. 24-1–24-15, Nov. 2003.
[26] M. Pan, E. F. Wood, D. B. McLaughlin, D. Entekhabi, and L. Luo, "A multiscale ensemble filtering system for hydrologic data assimilation. Part I: Implementation and synthetic experiment," *J. Hydrometeor.*, vol. 10, no. 3, pp. 794–806, Jun. 2009.
[27] M. Pan and E. F. Wood, "A multiscale ensemble filtering system for hydrologic data assimilation. Part II: Application to land surface modeling with satellite rainfall forcing," *J. Hydrometeor.*, vol. 10, no. 6, pp. 1493–1506, Dec. 2009.
[28] G. J. M. De Lannoy *et al.*, "Satellite-scale snow water equivalent assimilation into a high-resolution land surface model," *J. Hydrometeor.*, vol. 11, no. 2, pp. 352–369, Apr. 2010.
[29] H. Gao, E. F. Wood, M. Drusch, and M. F. McCabe, "Copula-derived observation operators for assimilating TMI and AMSR-E retrieved soil moisture into land surface models," *J. Hydrometeor.*, vol. 8, no. 3, pp. 413–429, Jun. 2007.
[30] J. Calvet and J. Noilhan, "From near-surface to root-zone soil moisture using year-round data," *J. Hydrometeor.*, vol. 1, no. 5, pp. 393–411, Oct. 2000.
[31] K. Mitchell *et al.*, "The multi-institution North American Land Data Assimilation System (NLDAS): Utilizing multiple GCIP products and partners in a continental distributed hydrological modeling system," *J. Geophys. Res. Atmos.*, vol. 109, no. D7, D07S90-1–D07S90-32, Apr. 2004.
[32] Y. Kerr *et al.*, "The SMOS soil moisture retrieval algorithm," *IEEE Trans. Geosci. Remote Sens.*, vol. 50, no. 5, pp. 1384–1403, May 2012.
[33] E. Jacquette *et al.*, "SMOS CATDS level 3 global products over land," in *Proc. Remote Sens. Agriculture, Ecosystems, Hydrology 11*, ser. Proc. SPIE-The Int. Soc. Opt. Eng., Neale, CMU and Maltese, A, Ed., vol. 7824, 2010, Conf. Remote Sens. Agriculture, Ecosyst., Hydrology 12, Toulouse, France, Sep. 20–22, 2010, pp. 1–6.
[34] X. Liang, D. Lettenmaier, E. Wood, and S. Burges, "A simple hydrologically based model of land-surface water and energy fluxes for general-circulation models," *J. Geophys. Res. Atmos.*, vol. 99, no. D7, pp. 14 415–14 428, Jul. 1994.
[35] X. Liang, E. Wood, and D. Lettenmaier, "Surface soil moisture parameterization of the VIC-2L model: Evaluation and modification," *Global Planet. Change*, vol. 13, no. 1–4, pp. 195–206, Jun. 1996.
[36] X. Liang, E. Wood, and D. Lettenmaier, "Modeling ground heat flux in land surface parameterization schemes," *J. Geophys. Res. Atmos.*, vol. 104, no. D8, pp. 9581–9600, Apr. 1999.
[37] E. P. Maurer, G. M. O'Donnell, D. P. Lettenmaier, and J. O. Roads, "Evaluation of the land surface water budget in NCEP/NCAR and NCEP/DOE reanalyses using an off-line hydrologic model," *J. Geophys. Res.*, vol. 106, no. D16, pp. 17 841–17 862, Aug. 2001.
[38] B. N. Nijssen, R. Schnur, and D. P. Lettenmaier, "Global retrospective estimation of soil moisture using the Variable Infiltration Capacity land surface model," *J. Clim.*, vol. 14, no. 8, pp. 1790–1808, Apr. 2001.
[39] J. Sheffield *et al.*, "Snow process modeling in the North American Land Data Assimilation System (NLDAS): 1. Evaluation of model-simulated snow cover extent," *J. Geophys. Res. Atmos.*, vol. 108, no. D22, pp. 10-1–10-13, Nov. 2003.
[40] J. Sheffield and E. F. Wood, "Global trends and variability in soil moisture and drought characteristics, 1950-2000, from observation-driven simulations of the terrestrial hydrologic cycle," *J. Clim.*, vol. 21, no. 3, pp. 432–458, Feb. 2008.
[41] B. Cosgrove *et al.*, "Real-time and retrospective forcing in the North American Land Data Assimilation System (NLDAS) project," *J. Geophys. Res. Atmos.*, vol. 108, no. D22, pp. 3-1–3-12, Oct. 31, 2003.
[42] M. Hansen, R. Defries, J. Townshend, and R. Sohlberg, "Global land cover classification at 1km spatial resolution using a classification tree approach," *Int. J. Remote Sens.*, vol. 21, no. 6/7, pp. 1331–1364, Apr. 15, 2000.
[43] G. Gutman and A. Ignatov, "The derivation of the green vegetation fraction from NOAA/AVHRR data for use in numerical weather prediction models," *Int. J. Remote Sens.*, vol. 19, no. 8, pp. 1533–1543, 1998.
[44] D. Miller and R. White, "A conterminous united states multilayer soil characteristics data set for regional climate and hydrology modeling," *Earth Interact.*, vol. 2, no. 1, pp. 1–26, Jan. 1998.
[45] K. Verdin and S. Greenlee, "Development of continental scale digital elevation models and extraction of hydrographic features," in *Proc., 3rd Int. Conf./Workshop Integrating GIS Environ. Model., Nat. Cent. Geogr. Inf. Anal.*, Santa Fe, New Mexico, 1996.
[46] M. Drusch, "Initializing numerical weather prediction models with satellite-derived surface soil moisture: Data assimilation experiments with ECMWF s Integrated Forecast System and the TMI soil moisture data set," *J. Geophys. Res.*, vol. 112, pp. D03102-1–D03102-14, Feb. 2007.
[47] V. R. N. Pauwels and G. J. M. De Lannoy, "Improvement of modeled soil wetness conditions and turbulent fluxes through the assimilation of observed discharge," *J. Hydrometeor.*, vol. 7, no. 3, pp. 458–477, Jun. 2006.
[48] M. J. van den Berg, S. Vandenberghe, B. De Baets, and N. E. C. Verhoest, "Copula-based downscaling of spatial rainfall: a proof of concept," *Hydrol. Earth Syst. Sci.*, vol. 15, no. 5, pp. 1445–1457, 2011.
[49] A. Sklar, "Fonctions de répartition à n dimensions et leurs marges," *Publ. Inst. Stat. Univ. Paris*, vol. 8, pp. 229–231, 1959.
[50] R. B. Nelsen, *An Introduction to Copulas*, New York, NY, USA: Springer-Verlag, 2006.
[51] J. Famiglietti, D. Ryu, A. A. Berg, M. Rodell, and T. J. Jackson, "Field observations of soil moisture variability across scales," *Water Resour. Res.*, vol. 44, no. 1, pp. W01423-1–W01423-16, Jan. 2008.
[52] H. Vernieuwe *et al.*, "Integrating coarse-scale uncertain soil moisture data into a fine-scale hydrological modeling scenario," *Hydrol. Earth Syst. Sci.*, vol. 15, no. 10, pp. 3101–3114, Oct. 2011.
[53] M. Pan, X. Yuan, and E. F. Wood, "A probabilistic view on drought recovery," *Geophys. Res. Lett.*, vol. 40, no. 14, pp. 3637–3642, 2013.
[54] C. Genest, J.-F. Quessy, and B. Rémillard, "Goodness-of-fit procedures for copula models based on the probability integral transformation," *Scand. J. Statist.*, vol. 33, no. 2, pp. 337–366, Jun. 2006.
[55] J. Fermanian, "Goodness-of-fit tests for copulas," *J. Multivariate Anal.*, vol. 95, no. 1, pp. 119–152, Jul. 2005.
[56] D. Huard, G. Evin, and A.-C. Favre, "Bayesian copula selection," *Comput. Statist. Data Anal.*, vol. 51, 2, pp. 809–822, Nov. 2006.

Niko E. C. Verhoest received the engineering and Ph.D. degrees in applied biological sciences from Ghent University, Ghent, Belgium, in 1994 and 2000, respectively.

During 1998–2000, he was a Teaching Assistant and during 2000–2002, he was an Assistant Professor with the Laboratory of Hydrology and Water Management, Ghent University. In 2002, he became an Associate Professor of hydrology and water management with the Faculty of Bioscience Engineering, Ghent University. His research interests include hydrological applications of radar remote sensing.

Martinus Johannes van den Berg received the bachelor's degree in nature and forestry management from Van Hall-Larenstein University, Leeuwarden, The Netherlands, in 2006, and the master's degree in earth sciences from the University of Amsterdam, Amsterdam, The Netherlands, in 2009. He is currently working toward the Ph.D. degree in hydrology and remote sensing at Ghent University, Ghent, Belgium.

Brecht Martens received the M.Sc. degree of Engineer in applied biological sciences from Ghent University, Ghent, Belgium, in 2012.

He is currently a Doctoral Research Assistant with the Laboratory of Hydrology and Water Management, Ghent University. His major research interest involves the use of remotely sensed hydrological variables to improve model simulations.

Hans Lievens received the Engineering and Ph.D. degrees in applied biological sciences from Ghent University, Ghent, Belgium, in 2007 and 2011, respectively.

Since 2011, he has been a Postdoctoral Research Fellow with the Research Foundation Flanders (FWO). His main research interests are soil moisture retrieval from active and passive microwave remote sensing, hydrologic modeling, and data assimilation.

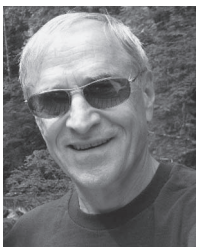

Eric F. Wood received the Susan Dod Brown Professorship in civil and environmental engineering from Princeton University, Princeton, NJ, USA, in 1976.

His research area is in hydroclimatology with an emphasis on the modeling and analysis of the global water and energy cycles through land surface modeling; satellite remote sensing of precipitation, soil moisture and evapotranspiration; and data analysis. Application areas include the monitoring and forecasting of drought, hydrologic impacts from climate change and seasonal hydrological forecasting.

Dr. Wood was the recipient of the Doctor Honoris Causa from Ghent University, Ghent, Belgium, in 2011, the 2014 Creativity Award of Prince Sultan Bin Abdulaziz International Prize for Water, European Geosciences Union's Alfred Wegener Medal and John Dalton Medal, AMS's Jules G. Charney Award and Robert E. Horton Memorial Lectureship, and the American Geophysical Union's Hydrology Section's Robert E. Horton Award. He is a Foreign Fellow of the Australian Academy of Technological Sciences and Engineering (ATSE), a Fellow of the Royal Society of Canada, the American Geophysical Union, and the American Meteorological Society.

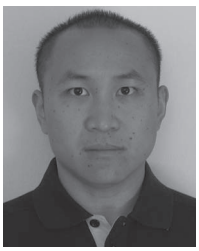

Ming Pan received the B.E. degree in hydraulic engineering from Tsinghua University, Beijing, China, in 2000, the M.A. and Ph.D. degrees in civil and environmental engineering from Princeton University, Princeton, NJ, USA, in 2002 and 2006, respectively.

From 2006 to 2007, he performed postdoctoral research in the area of data assimilation at Princeton University and the Massachusetts Institute of Technology, Cambridge, MA, USA. He is currently a Research Scholar with the Department of Civil and Environmental Engineering, Princeton University.

Dr. Pan is a member of the American Geophysical Union and American Meteorological Society.

Yann H. Kerr (M–88–SM'01–F'13) received the Engineering degree from the Ecole Nationale Supérieure de l'Aéronautique et de l'Espace, the M.Sc. degree in electronics and electrical engineering from Glasgow University, Glasgow, Scotland, U.K., and the Ph.D. degree in Astrophysique Geophysique et Techniques Spatiales, Université Paul Sabatier, Toulouse, France.

His fields of interest are in the theory and techniques for microwave and thermal infrared remote sensing of the Earth, with emphasis on hydrology, water resources management. He was an EOS Principal Investigator (PI) (interdisciplinary investigations) and PI and precursor of the use of the SCAT over land. In 1988, he started to work on the interferometric concept applied to passive microwave Earth observation and was subsequently the science lead on the MIRAS project for the European Space Agency. In 1997, he proposed the Soil Moisture and Ocean Salinity (SMOS) Mission, the natural outcome of the previous MIRAS work. He is currently the Director of Centre d'études Spatiales de la BIOsphère, Toulouse, France. He is currently involved in the exploitation of SMOS data, in the calibration/validation activities and related level 2 soil moisture and level 3 and 4 developments. He is also working on the SMOS next concept and involved in both the Aquarius and SMAP missions.

Dr. Kerr received the First Prize World Meteorological Organization (Norbert Gerbier), the U.S. Department of Agriculture Secretary's Team Award for Excellence (Salsa Program), the Geoscience and Remote Sensing Society (GRSS) certificate of recognition for leadership in development of the first synthetic aperture microwave radiometer in space, and success of the SMOS mission, and is a Distinguished Lecturer for GRSS.

Ahmad Al Bitar received the B.A. degree from the Lebanese University, Beirut, Lebanon, and the M.E. degree in from the Institut National des Sciences Appliquées (INSA-Lyon), France in 2003, both in civil engineering. He received the Ph.D. degree from the Institut National Polythechnique de Toulouse, Toulouse, France in hydrogeology in 2006. His thesis work focused on numerical modeling in stochastic porous media in the context of surface/subsuface coupling.

In 2006, he joined the Centre d'Études Spatiales de la BIOsphère (CESBIO), France as a Research Fellow on integrated hydrological modeling. Since 2008, he has been with the Soil Moisture and Ocean Salinity (SMOS) mission team. He contributed to the SMOS commissioning phase, the calibration/validation activities, and the definition of L3 multiorbit SMOS products. He is working on high end level 4 products from the SMOS mission. His main areas of interest are assimilation of remote sensing data more specifically from microwave sensors into integrated hydrological modeling.

Sat K. Tomer received the M.E. degree in water resources and environmental engineering from the Indian Institute of Science, Bangalore in 2008. He received Ph.D. degree from the Indian Institute of Science, Bangalore and is currently working as a Postdoctoral Fellow with the Centre d'Études Spatiales de la Biosphere, Toulouse, France.

His research interests include retrieval of hydrological variables from remote sensing and assimilation of remote sensing products into hydrological models.

Matthias Drusch received the Diploma degree from Kiel University, Kiel, Germany, in 1994, the Ph.D. degree from Bonn University, Bonn, Germany, in 1998, and the Habilitation in Meteorology from Bonn University, Bonn, in 2011.

He was with Princeton University, Princeton, NJ, USA, and Bonn University before joining the European Centre for Medium-Range Weather Forecasts from 2002 to 2008. Since 2008, he has been with the European Space Agency (ESA) as the Land Surfaces Principal Scientist in the Mission Science Division. His fields of interest are in remote sensing and radiative transfer modeling, data assimilation, hydrological modeling, and weather forecasting. He is currently the Mission Scientist for Sentinel-2, the Fluorescence Explorer Earth Explorer 8 candidate mission, and ESA's Soil Moisture and Ocean Salinity Science and Applications Representative.

Dr. Drusch is a member of the American Geophysical Union and the Deutsche Meteorologische Gesellschaft.

Hilde Vernieuwe was born in 1977. She received the Engineering and Ph.D. degrees in applied biological sciences from Ghent University, Ghent, Belgium, in 2000 and 2005, respectively.

In January 2001, she joined KERMIT, the research unit *Knowledge-Based Systems*, Ghent University, to conduct research in the fields of fuzzy modeling and hydrology. Since January 2007, she has been a Postdoctoral Researcher with KERMIT, Department of Mathematical Modelling, Statistics and Bioinformatics, Ghent University.

Bernard De Baets received the M.Sc. degree in mathematics in 1988, the Postgraduate degree in knowledge technology in 1991, and the Ph.D. degree in mathematics in 1995 (all *summa cum laude*).

During 1988–89, he was a Government of Canada Award Holder with the Intelligent Systems Research Laboratory of the University of Saskatchewan, Saskatoon, Saskatchewan. In 2006, he was an Honorary Professor of Budapest Tech (Hungary). In 2008, he became a Full Professor in applied mathematics at Ghent University, Ghent, Belgium, where he is leading the research unit Knowledge-based Systems (KERMIT, 2000) at the Faculty of Bioscience Engineering. In 2009, he was an Affiliated Professor with the Anton de Kom Universiteit (Suriname). His bibliography comprises more than 370 publications in international peer-reviewed journals, 60 chapters in books, and 270 contributions to proceedings of international conferences. He acted as supervisor of over 50 Ph.D. students and delivered over 200 lectures at conferences and research institutes.

Dr. De Baets was the recipient of several best paper awards (1994, 2006, 2007, 2009, 2010, 2013, 2015). He is a Co-editor-in-Chief (2007) of *Fuzzy Sets and Systems* and a member of the editorial board of several other journals. He was elected Fellow of the International Fuzzy Systems Association in 2011 and has been nominated for the 2012 Ghent University Prometheus Award for Research.

Jeffrey P. Walker received the B.E. (Civil) and B.Surveying degrees in 1995 (with first-class honors) and the University Medal from the University of Newcastle, Australia, Callaghan, N.S.W., Australia, and the Ph.D. degree in water resources engineering from the same university in 1999. His Ph.D. thesis was among the early pioneering research on estimation of root-zone soil moisture from assimilation of remotely sensed surface soil moisture observations.

He then joined the NASA Goddard Space Flight Center to implement his soil moisture work globally. In 2001, he moved to the Department of Civil and Environmental Engineering at the University of Melbourne as Lecturer, where he continued his soil moisture work, including development of the only Australian airborne capability for simulating new satellite missions for soil moisture. In 2010, he was appointed as Professor in the Department of Civil Engineering at Monash University where he is continuing this research. He is contributing to soil moisture satellite missions at NASA, ESA, and JAXA, as a Science Team member for the Soil Moisture Active Passive (SMAP) mission and Cal/Val Team member for the Soil Moisture and Ocean Salinity (SMOS) and Global Change Observation Mission—Water (GCOM-W), respectively.

Gift Dumedah received the B.Sc. degree (with honors) in geodetic engineering from Kwame Nkrumah University of Science and Technology, Kumasi, Ghana in 2002 with a thesis entitled: A geographical information system for the Ghana Army. He received the M.Sc. degree in geography from Simon Fraser University, Vancouver, BC, Canada, in 2005, with a specialization in geographic information science. He received the Ph.D. degree in geography in 2010 from the University of Guelph, Guelph, ON, Canada, with a thesis titled: multiobjective calibration of hydrological models and data assimilation using genetic algorithms. This was followed by a year and a half long Postdoctoral Fellowship with the School of Geography and Earth Sciences at McMaster University, Canada.

In October 2011, he joined the Department of Civil Engineering at Monash University in Melbourne, Melbourne, Vic., Australia, where he is contributing to soil moisture research for sustainable land and water management. His research focus is on integrated assessment of climate variability and human impact on sustainable water resources by employing advanced land surface monitoring strategies for efficient observation-model synthesis. Specific primary interests include observation-model synthesis, data assimilation, evolutionary computation, and remote sensing and GIScience applied to water resources.

Valentijn R. N. Pauwels received the M.Sc. degree of Engineer in agricultural sciences from Ghent University, Ghent, Belgium, in 1994. In 1999, he received the Ph.D. degree in civil engineering and operations research from Princeton University, Princeton, NJ, USA.

From 1999 to 2004, he was a Postdoctoral Research Fellow funded by the Foundation for Scientific Research of the Flemish Community. He undertook this position at Ghent University, at which he became a Lecturer in 2005 and a Senior Lecturer in 2010. In 2012, he moved to Monash University, where he is currently an Associate Professor. He is currently a Future Fellow funded by the Australian Research Council. His major research interest is hydrologic model development and optimization.